energy&fuels

pubs.acs.org/EF

Article

Electric Fields Assisted ZIF-8 Adsorption Hydration Methane Storage and Release: A Molecular Insight

Published as part of Energy & Fuels special issue "2025 Pioneers in Energy Research: E. Dendy Sloan".

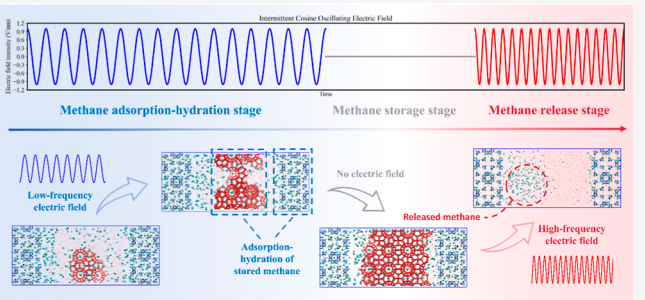
Changle Li, Shuanshi Fan,* Yanhong Wang, Xuemei Lang, and Gang Li

Cite This: *Energy Fuels* 2026, 40, 2571−2581

Read Online

ACCESS | Metrics & More | Article Recommendations | Supporting Information

ABSTRACT: The ZIF-8 adsorption-hydration method is regarded as a highly promising technology for methane storage. However, the high temperatures required for ZIF-8 desorption and the slow growth rate of methane hydrate has become unsatisfactory in current production. In this study, the behavior of ZIF-8 adsorption-hydration for methane storage and release under a cosine-oscillating electric field was systematically investigated via molecular dynamics simulations. The results indicate that an electric field of 1 V/nm at 8 THz can effectively promote methane desorption from ZIF-8. Under 273 K and 0.1 MPa, the residual fraction of methane in ZIF-8 after desorption decreased from 77.7% to 5.4%. In addition, the electric field influences hydrate growth by modulating hydrogen bonding between water molecules, and, at each field strength, there is a frequency window that promotes hydrate formation. High-frequency fields disrupt the hydrogen bonds within the hydrate phase, accelerating decomposition. Fields with suitable frequency disrupt hydrogen bonds in the liquid, improving gas−liquid interaction and facilitating hydrate formation. By applying an intermittent electric field of 1 V/nm at 4 THz, high-speed, stable methane-hydrate growth was achieved, with a growth rate five times that of a control system without an electric field. These findings elucidate, at the molecular scale, the mechanism by which a cosine-oscillating electric field governs methane storage and release in the ZIF-8 adsorption-hydrate method and provide theoretical guidance for developing efficient methane storage and transport technologies.

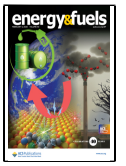


1. INTRODUCTION

The world is currently facing the dual challenges of energy crisis and climate change. Green energy, such as solar,[1] wind,[2] wave,[3] and hydrogen energy,[4] will gradually replace fossil energy as the "power of the future". However, because these renewable energy solutions still fall short of sustainable economic needs,[5] natural gas—being the lowest-emission fossil fuel—has arisen as a crucial transitional energy source. As a fundamental part of the world's energy mix, natural gas is extensively utilized in electricity generation, industrial processes, home heating, and to augment combustion.[6−8] However, the growth of natural gas energy demand, considering its seasonal and demand-driven consumption fluctuations, efficient and safe storage and transportation technologies must be developed in order to ensure its supply stability.[9] Recent investigations demonstrate that encapsulating methane within hydrate structures is both safe and practical.[10] Methane hydrates are nonstoichiometric, cage-like crystals generated when water and methane interact under low temperatures and high pressures.[11] H_2O hydrogen-bonds together, creating cage-like networks that encapsulate methane.[12] Nevertheless, the sluggish hydrate growth kinetics restrict their practical industrial use.

To accelerate the growth kinetics of methane hydrate, researchers introduced the adsorption-hydration approach. While enhancing the growth kinetics of the hydration process, it also improves its gas storage capacity.[13−16] Compared with the adsorption technique, the adsorption hydration approach enhances the gas storage capacity by preadsorbing an appropriate amount of water to form hydrates under certain conditions.[17] A range of porous substrates, among them metal−organic frameworks (MOFs), have demonstrated great potential for promoting hydrate formation,[18−20] due to their large surface areas and adjustable pore structures.[21,22] Mu et al.[23] first introduced adsorbed water into ZIF-8 in 2012, revealing that over half of the stored methane was present as hydrates. Meanwhile, it has been shown that HKUST-1[24,25] and ZIF-8[26] can significantly shorten the hydrate induction

Received: October 15, 2025
Revised: January 10, 2026
Accepted: January 12, 2026
Published: January 26, 2026



Downloaded from pubs.acs.org/enfuem/article-pdf/40/5/2571/6332305/ef5c05447.pdf by SOUTH CHINA UNIV OF TECHNOLOGY user on 02 November 2026

© 2026 American Chemical Society

https://doi.org/10.1021/acs.energyfuels.5c05447
Energy Fuels 2026, 40, 2571−2581

time and increase the water conversion rate to more than 85%. Factors such as the pore size and surface properties of MOFs have an important influence on the ability of adsorption-hydration for methane storage. Kim et al.[27] found that it is difficult to form hydrate in the micropores filled with water in MOFs, which is limited by the size of hydrate cells and the confinement effect of micropores. Additionally, hydrophilic MOFs can block pores with water,[23,27] hindering methane adsorption. In contrast, Casco et al. found that[28] hydrophobic MOFs like ZIF-8 prevent water molecules from entering their cavities, preserving methane adsorption capacity. Zhang et al.[29] observed that a hydrophobic surface aids methane dissolution in water, thereby encouraging hydrate formation. Hydrate formation within interparticle voids and atop ZIF-8 surfaces leads to markedly higher methane uptake compared to the anhydrous ZIF-8.[28] In fact, the adsorption hydration approach suffers from the problem of harsh conditions and a low rate of methane release, and the desorption of methane by ZIF-8 often requires high temperatures of several hundred degrees, while the decomposition of hydrates, although under mild conditions, has an unsatisfactory decomposition rate. Moreover, applying an external electric field offers an effective solution to this issue.

Besides using porous materials to accelerate hydrate formation kinetics, applying an external electric field has been shown to effectively stimulate hydrate growth.[30−33] Common forms of electric fields include static electric fields, pulsed electric fields, and cosine oscillating electric fields. Studies by Zhou[34] and Liang[35] have shown that both static and pulsed electric fields can disrupt hydrate structures. In contrast, Shi et al.[36] reported that a cosine oscillating electric field with an appropriate oscillation frequency and field strength can promote the rapid growth of methane hydrates. This effect stems from the electric field's capacity to reorient H_2O, aligning them closer to the typical geometric configuration of hydrate lattices.[37] Luis et al.[38] found that applying a suitable electric field can elevate the coexistence temperature among gas, liquid, and hydrate phases, thereby improving hydrate stability. Shi et al.[36] found that the hydrate growth rate reaches three times that of the system without an electric field under a 1.5 V/nm, 0.4 THz cosine oscillating electric field. This effect was linked to the electric field's enhancement of hydrogen bond formation. Moreover, hydrate decomposition can occur when the field's strength or frequency surpasses a specific threshold.[39−42] This is attributed to the electric field disrupting hydrogen bonds, triggering a rearrangement of water molecules.[43−46] Fang[47] and Liang[35] also suggested that the electric field under certain conditions can resonate with H_2O, which destroys the hydrogen bonds in the hydrates and accelerates the decomposition of hydrates.

By tuning the electric-field conditions, one can simultaneously enhance hydrate growth kinetics and achieve its rapid decomposition. In this work, the molecular behavior of ZIF-8 adsorption-hydration storage of methane under a cosine oscillating electric field was investigated, and the effects of key parameters such as electric field strength and frequency on the adsorption characteristics of ZIF-8 and hydrate growth behavior were discussed. A cosine oscillating electric field has been demonstrated to enhance the rate of methane adsorption-hydration storage in ZIF-8. Furthermore, altering the electric field conditions can facilitate the efficient release of methane. This offers a practical solution to overcome the major challenges in applying adsorption-hydration methane storage technology.

2. MODELS AND SIMULATION METHODS

ZIF-8 consists of zinc ions connected to 2-methylimidazole molecules by tetrahedral coordination. Each zinc ion forms a Zn−N bond with four nitrogen atoms of imidazole, constituting a three-dimensional backbone of the soda-lime-like topology, which contains regularly arranged cavities and connecting channels of about 3.4 Å to form a stable periodic microporous network.[48] In addition, intergranular pores exist between ZIF-8 particles,[27] which provide a suitable region for methane hydrate formation. On this basis, the ZIF-8 physisorption and ZIF-8 intergranular hydration for methane storage were modeled in this study. A single ZIF-8 cell was first 5 × 2 × 2 supercelled,[49] while the intermediate 3 × 2 × 2 ZIF-8 was later deleted to construct intergranular pores. In the ZIF-8 adsorption-hydration process, methane exhibits bidirectional convective behavior.[50] If ZIF-8 did not preadsorb methane, methane would enter the ZIF-8 cavity during hydration and inhibit hydrate formation.[51] In contrast, after preadsorption of methane, ZIF-8 was able to provide methane to promote hydrate formation during hydration.[29] Therefore, the simulation of methane adsorption by ZIF-8 was carried out at 260 K and 10 MPa for 50 ns. And then the unadsorbed methane in the intergranular pores was removed to obtain the adsorption-saturated ZIF-8 for subsequent modeling. Furthermore, water scarcity makes adsorption and hydration strongly compete; once water is ample, gas uptake by ZIF-8 instead accelerates hydrate growth.[52] Therefore, in this study, the water content was set to be 2 × 2 × 2 methane hydrate cells were placed in the ZIF-8 intergranular pores, and 193 CH_4 and 1144 H_2O were randomly inserted in the blank area to complete the construction of the initial model, as shown in Figure 1. The left and right sides of the box are ZIF-8, with ZIF-8 intergranular pores in the center.

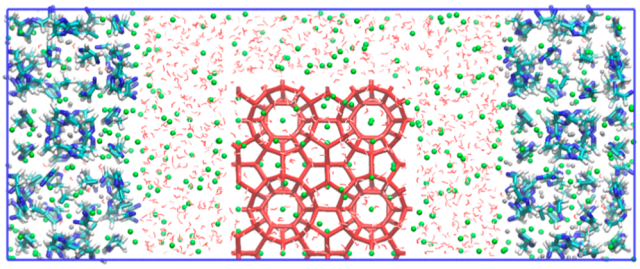


Figure 1. Snapshot of the initial model for the simulation. Red stick: methane hydrate, green ball: methane molecule, red line: water molecule, white, cyan, blue, and gray represent H, C, N, and Zn atoms in ZIF-8, respectively.

All molecular dynamics simulations employed GROMACS 2023.3 with periodic boundary conditions along the three spatial dimensions. The force field files of ZIF-8 were generated by the Sobtop software package,[53] and the UFF and GAFF force fields were used for their description. And then the periodic ZIF-8 atoms were subjected to REPEAT charge calculations using the CP2K software package, which reproduces the electrostatic potential of the periodic system very well.[54] The TIP4P/Ice[55] and TraPPE joint atomic force fields[56] were used for H_2O and CH_4, respectively, with the LINCS algorithm constraining all system bonds. The Lorentz−Berthelot mixing rule calculated the cross-interaction Lennard-Jones potential parameters for the atoms. The Long-range electrostatic interactions[57] were calculated using the Ewald (PME) method, with a Fourier grid spacing of 0.14 nm. The simulation process started with an energy minimization of the system, which was followed by a pre-equilibrium simulation of *NVT* at 1 ns and *NPT* at 10 ns. The structure was relaxed until both temperature and pressure stabilized. During the *NVT* simulation, the location of methane hydrate was frozen to prevent hydrate seed decomposition. Finally, an 800 ns *NPT*

Downloaded from pubs.acs.org/enfuem/article-pdf/40/5/2571/6332305/ef5c05447.pdf by SOUTH CHINA UNIV OF TECHNOLOGY user on 02 November 2026

https://doi.org/10.1021/acs.energyfuels.5c05447
Energy Fuels 2026, 40, 2571−2581

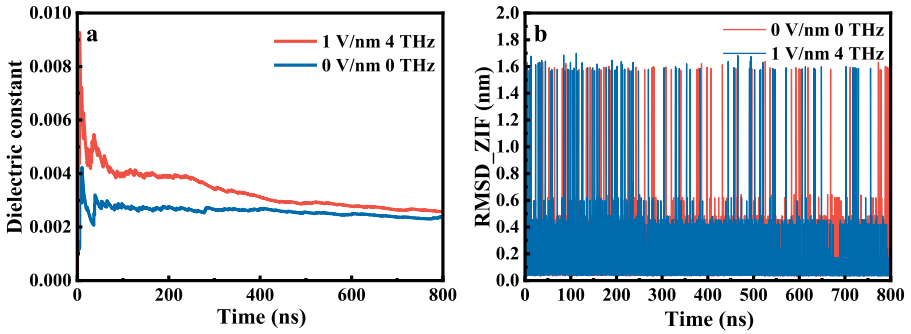


Figure 2. Comparison of structural properties of ZIF-8 without applied electric field and with applied 1.0 V/nm, 4.0 THz electric field conditions: (a) dielectric constant, (b) root-mean-square deviation.

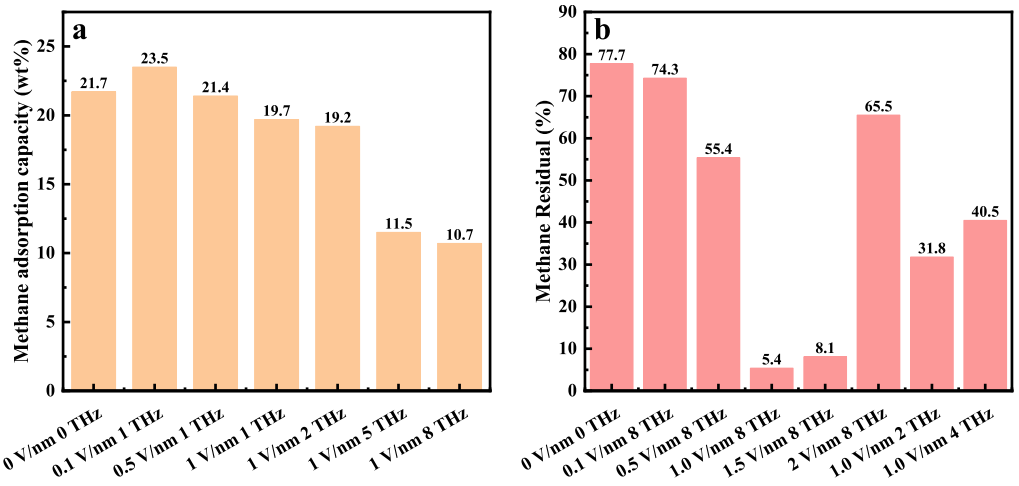


Figure 3. Effect of methane adsorption and desorption by ZIF-8 under different electric field conditions: (a) mass fraction of methane adsorbed by ZIF-8 at 273 K, 10 MPa, and different electric field conditions, and (b) percentage of methane remaining after desorption by ZIF-8 at 273 K, 0.1 MPa, and different electric field conditions.

simulation was performed at the specified temperature and pressure. Simulations used a Nose−Hoover thermostat (τ = 2 ps) and a Parrinello−Rahman barostat (τ = 4 ps); the equations of motion were integrated using the leapfrog scheme with a 2 fs time step. In addition, during the *NPT* simulations, a cosine oscillating electric field was applied along the *x*, *y*, and *z* directions of the simulation box. Unless otherwise stated, the electric-field strength reported hereafter refers to the single-axis field amplitude E_0. The resultant total field magnitude is $E_{total} = \sqrt{3}\ E_0$. In addition, a positional constraint of 1000 kJ/mol was applied to the ZIF-8 atoms to ensure that the structure of ZIF-8 would not be severely damaged.

3. RESULTS AND DISCUSSION

3.1. Effect of Electric Field on Adsorption and Desorption of Methane by ZIF-8

This molecular dynamics simulation examines how cosine oscillating electric fields affect the structure of ZIF-8, calculating the dielectric constant and root-mean-square deviation of its atoms under a field of 1.0 V/nm and 4.0 THz, as shown in Figure 2. As shown in Figure 2a, the fluctuation in the dielectric constant of ZIF-8 increased significantly upon applying the electric field, which led to polarization effects altering the electrostatic interaction forces between the molecules and prompting structural adjustments and adaptations in ZIF-8. The dielectric constant stabilizes after 400 ns, suggesting that the electric field gradually stabilizes the ZIF-8 structure. The root-mean-square deviation results show that while electric fields improve the stability of ZIF-8, it requires a response time to fully manifest, as depicted in Figure 2b. This is consistent with the time of dielectric constant stabilization. The radial distribution function of each atom in ZIF-8 under an electric field in Figure S1 further reveals the change of the ZIF-8 structure. Since H, C, and N atoms are more easily polarized, the concentration of these atoms in the short-range region is higher under the action of the electric field. While Zn atoms have strong electronegativity, the polarization effect is weaker. Therefore, the electric field primarily redistributes the Zn electron cloud, leading to a more diffuse arrangement of Zn atoms.

Changes in the structure of ZIF-8 may directly affect its adsorption and desorption behavior of CH_4. In particular, the electric field modified the microstructure of ZIF-8, thereby altering its adsorption performance. To clarify this effect, the adsorption behavior of ZIF-8 on CH_4 was simulated separately in this study. Figure 3a demonstrates the adsorption capacity of ZIF-8 for methane under different electric field conditions. A promoting effect on CH_4 adsorption by ZIF-8 was observed only at an electric field of 0.1 V/nm and 1.0 THz. Under all other electric field conditions, the adsorption of CH_4 by ZIF-8 was inhibited to some extent. The inhibition progressively intensified as the electric field strength and frequency increased. The two opposing outcomes primarily arise from the regulation of methane kinetics and residence time by the electric field. At relatively low field strengths, the field oscillation and weak polarization effects enhance methane

https://doi.org/10.1021/acs.energyfuels.5c05447
Energy Fuels 2026, 40, 2571−2581

Downloaded from pubs.acs.org/enfuem/article-pdf/40/5/2571/6332305/ef5c05447.pdf by SOUTH CHINA UNIV OF TECHNOLOGY user on 02 November 2026

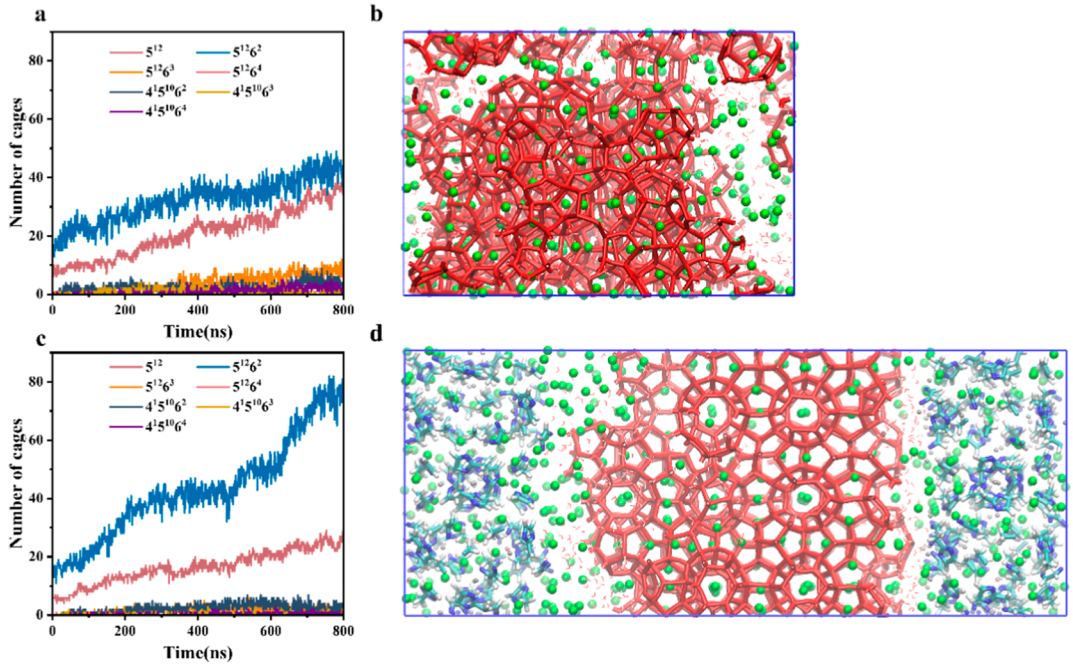


Figure 4. Snapshots of the number of hydrate cages with/without the ZIF-8 system over time and modeling at 800 ns: (a,b) without the ZIF-8 system, and (c,d) with the ZIF-8 system. Red stick: methane hydrate, blue ball:H_2O (only O shown), green ball: CH_4.

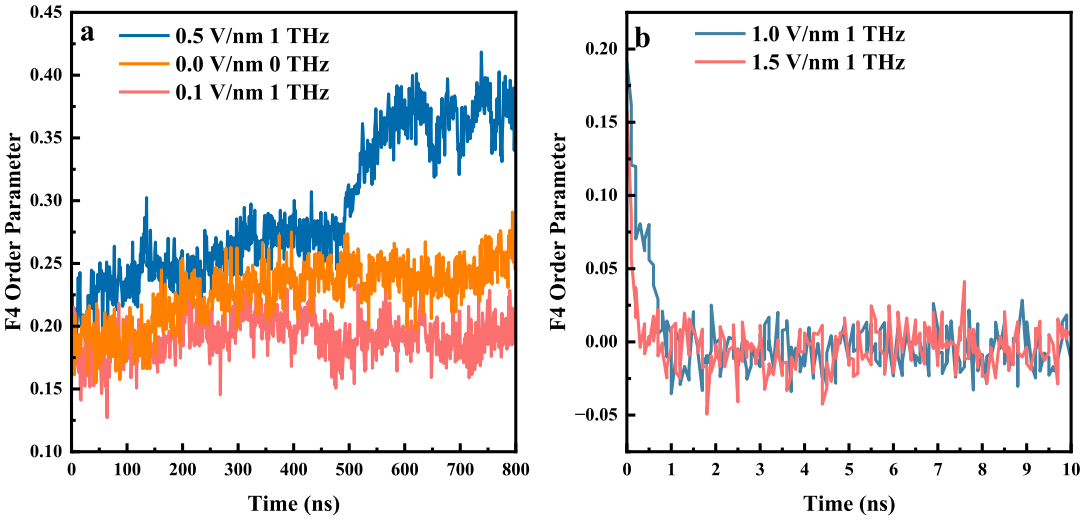


Figure 5. Variation of F4 order parameters of the system at different electric field strengths: (a) 0, 0.1, 0.5 V/nm, (b) 1.0, 1.5 V/nm.

kinetics, allowing more methane to enter ZIF-8 during the period of field application. However, as the field strength increases, methane kinetics are further intensified, which shortens the residence time of methane molecules in ZIF-8 and consequently leads to a greater tendency for methane molecules to escape. When the intergranular pores of ZIF-8 filled with H_2O and formed hydrates, the CH_4 adsorption remained unchanged, with the potential for even higher methane adsorption, as illustrated in Figure S2. This is attributed to the hydrophobicity of ZIF-8 and the "closing" effect of the hydrate on the ZIF-8 cavity, which resulted in the formation of localized CH_4 bubbles with high concentration on the ZIF-8 surface, leading to the increase of adsorption driving force. This counteracted the field's inhibitory impact on CH_4 adsorption by ZIF-8. Building on the electric field's inhibition of CH_4 adsorption by ZIF-8, its influence on CH_4 desorption was also studied at 273 K and 0.1 MPa. Figure S3 shows the variations in methane adsorption by ZIF-8 under various electric field conditions. This means that applying an electric field significantly enhances methane desorption from ZIF-8. Figure 3b illustrates the residual methane rate within ZIF-8 across various electric field conditions. Under no electric field conditions, 77.7% of CH_4 inside the ZIF-8 cavity could not be released. This is a major shortcoming of adsorption storage of methane using porous materials such as ZIF-8, where better desorption can only be achieved under high-temperature conditions. This energy-intensive storage method is not suitable for large-scale industrial applications. Following the electric field application, the residual CH_4 in the ZIF-8 cavity decreased significantly, particularly at 1.0 V/nm and 8.0 THz; the final residual CH_4 was only 5.4%, which significantly improved the desorption efficiency of ZIF-8, and These

https://doi.org/10.1021/acs.energyfuels.5c05447
Energy Fuels 2026, 40, 2571−2581

Downloaded from pubs.acs.org/enfuem/article-pdf/40/5/2571/6332305/ef5c05447.pdf by SOUTH CHINA UNIV OF TECHNOLOGY user on 02 November 2026

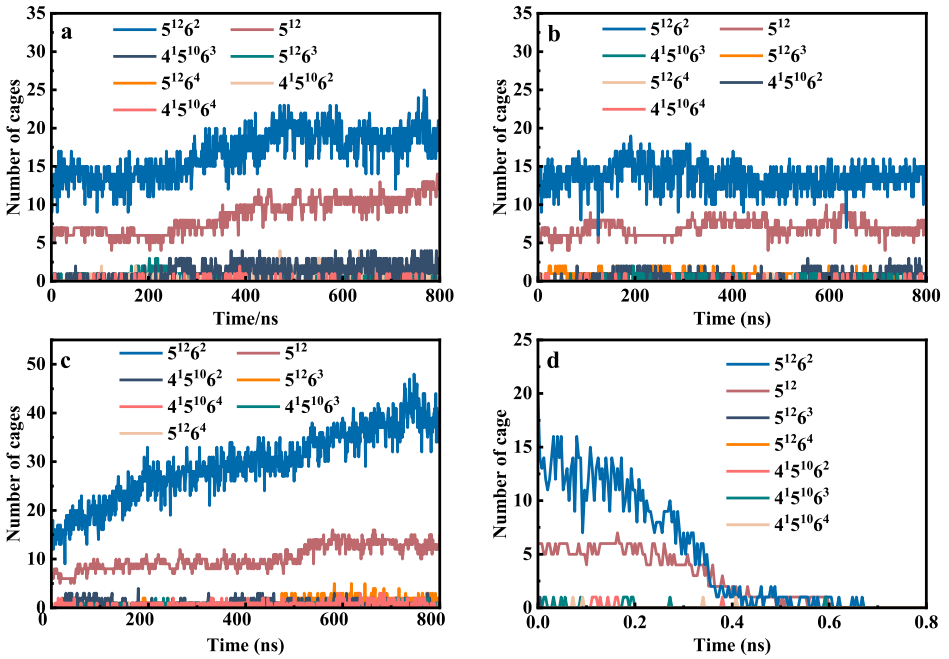


Figure 6. Variation of the number of hydrate cages with time for the simulation processes (a) 0 V/nm, 0 THz, (b) 0.1 V/nm, 1.0 THz, (c) 0.5 V/nm, 1.0 THz, and (d) 1.0 V/nm, 1.0 THz.

findings offer a promising approach for low-energy methane storage and release.

3.2. Effect of Electric Field Strength on the Growth of ZIF-8 Intergranular Methane Hydrate

Another important part of the adsorption hydration approach for methane storage is the growth of ZIF-8 intergranular methane hydrate. To clarify the effects of ZIF-8 and cosine oscillating electric field on hydrate growth, the growth process of ZIF-8 intergranular hydrate was first simulated at 260 K and 30 MPa. Figure 4a and 4c illustrate the variations in cage numbers throughout the growth of the bulk system and ZIF-8 intergranular hydrate. The growth rate of ZIF-8 intergranular hydrate reached 170% of the bulk system. This phenomenon arises from the two-way nanoconvection convection of ZIF-8 within its intergranular pores, enhancing CH_4 and H_2O diffusion rates, as illustrated in Figure S4. Figure 4b and 4d shows snapshots of the simulation at 800 ns for the system without and with ZIF-8. In the bulk system, methane hydrate undergoes noticeable displacement and rotation. In contrast, the constraining effect of ZIF-8 restricts the movement of the hydrate and makes its arrangement more orderly, which may be beneficial to the stable preservation of the hydrate.

To better observe the electric field effect, molecular dynamics simulations were conducted under constant conditions of 260 K and 10 MPa, with five systems exposed to field strengths of 0, 0.1, 0.5, 1.0, and 1.5 V/nm. As shown in Figure 5a, the F4 order parameters of the intergranular portion of ZIF-8 for the five systems were first calculated. The cosine oscillating electric field at 0.5 V/nm was found to improve the system's order. In particular, at approximately 500 ns, the F4 order parameter increased rapidly, and the hydrate growth rate was correspondingly enhanced. This indicates that the electric field influences hydrate growth through an induction process, in which water molecules require a certain period of time to adapt to the oscillation frequency of the applied field. Once the water molecules have adapted to the field oscillation, the water in the system becomes more ordered, which in turn further promotes the rapid formation of hydrates. Specific electric field frequency and electric field strength under H_2O orderly arrangement thus promote the formation of hydrate. At 0.1 V/nm electric field, H_2O may be subject to the dual action of coulomb force and intermolecular force; some of the forces cancel each other instead of inhibiting the movement and orderly arrangement of H_2O. In addition, the 1.0 and 1.5 V/nm electric fields significantly disrupted the ordering of H_2O within the intergranular pores of ZIF-8, as demonstrated in Figure 5b. The F4 order parameter was reduced from 0.2 to below 0 within 1.0 ns, which is almost close to the F4 order parameter of liquid water. This implies that the initially placed hydrate seed structure is disrupted, suggesting that the excessive electric field strength is likely to drive the decomposition of the hydrate.

To analyze the growth behavior of ZIF-8 intergranular hydrate, the number of hydrate cages during the simulation was calculated, as shown in Figure 6a–c. On the contrary, the hydrate in the system with the applied 0.5 V/nm electric field maintains a stable and high-speed growth. It can be seen that in this electric field, conditions can effectively promote the formation of hydrate. And the electric field mainly promotes the formation of the $5^{12}6^2$ large cages, which indicates that the electric field conditions help to stabilize the $5^{12}6^2$ cages. The selective promotion of the $5^{12}6^2$ cage by an electric field arises from the greater stability of its hydrogen-bond network and the field-induced orientational ordering of water molecules, which favors the assembly of such stable structures. The 5^{12} and $5^{12}6^2$ cages are representative cage types in sI hydrates, consisting of regular pentagonal and hexagonal rings. Water molecules in these cages form a complete tetrahedral hydrogen-bond network, resulting in relatively high structural stability. In contrast, noncanonical cages such as $5^{12}6^3$ often contain incomplete hydrogen-bond connectivity; they typically appear only transiently during the early stage of hydrate nucleation and are considered metastable structures.[58] Previous studies

Downloaded from pubs.acs.org/enfuem/article-pdf/40/5/2571/6332305/ef5c05447.pdf by SOUTH CHINA UNIV OF TECHNOLOGY user on 02 November 2026

https://doi.org/10.1021/acs.energyfuels.5c05447
Energy Fuels 2026, 40, 2571−2581

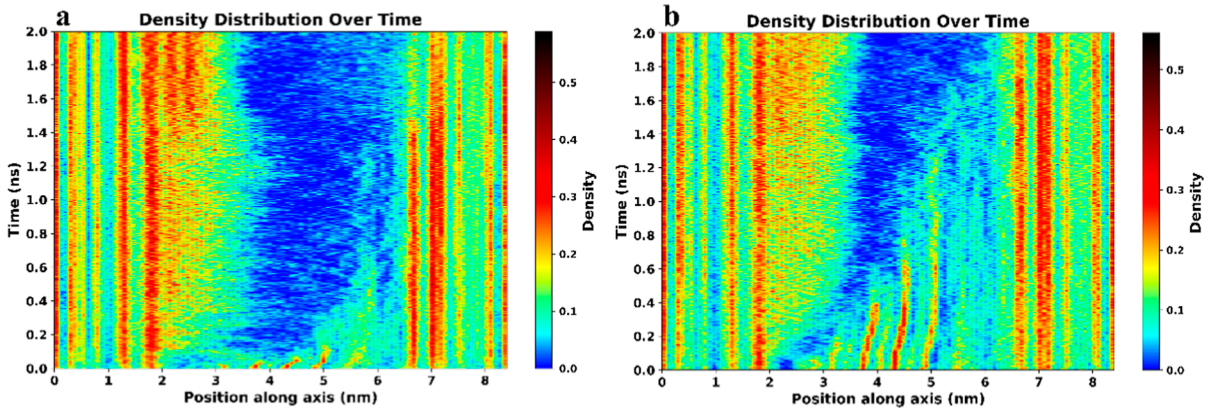


Figure 7. Density distribution of CH_4 in the *x*-direction with time: (a) 1.0 V/nm, 1.0 THz; (b) 1.5 V/nm, 1.0 THz.

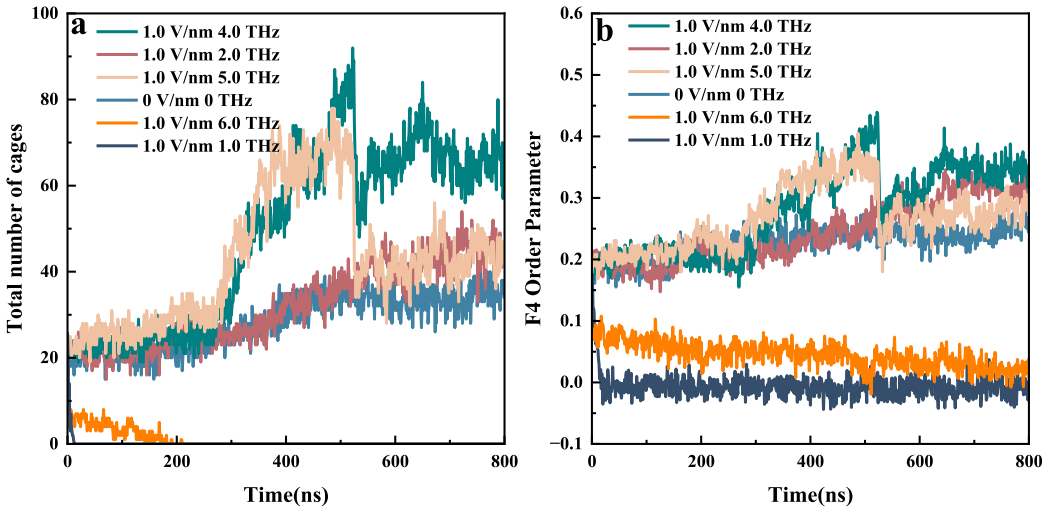


Figure 8. Variation of total hydrate cage number and F4 order parameter with time for different electric field frequencies. (a) Total hydrate cage number, (b) F4 order parameter.

have shown that an electric field can align the dipole moments of water, inducing a more directional hydrogen-bond network.[59] Under an electric field of appropriate strength, collective water vibrations may resonate with the applied field, causing repeated rupture and reformation of hydrogen bonds.[60] Moreover, strong electric fields have been reported to strengthen hydrogen bonding and drive the hydrogen-bond network toward ice-like hexagonal-ring configurations.[61] Therefore, the electric field tends to disrupt metastable local hydrogen-bond motifs and enables water molecules to rearrange into a lower-energy, ordered ring network, thereby preferentially promoting the formation of the more stable $5^{12}6^2$ cages. And it can be observed that the number of non-sI-type hydrate cages other than 5^{12} and $5^{12}6^2$ cages is significantly reduced in the electric field system with 0.1 and 0.5 V/nm applied. This suggests that hydrate cages generated in the presence of an electric field maintain greater structural stability and are less prone to transformation. As shown in Figure 6d, an electric field intensified to 1.0 V/nm induces a marked change in hydrate growth behavior, characterized by accelerated decomposition. The decomposition behavior of the hydrate under a strong electric field of 1.0 V/nm shows two phases: (1) the $5^{12}6^2$ cage decomposes first until it coincides with the number of 5^{12} cages, and (2) the 5^{12} and $5^{12}6^2$ cages decompose simultaneously. This indicates that the 5^{12} cage exhibits greater stability than the $5^{12}6^2$ cage at high electric field strengths.

To clarify the decomposition behavior of hydrate under a strong electric field, the CH_4 density distribution in the *x*-direction was further analyzed, as shown in Figure 7. Under different electric field strengths, the hydrate exhibits different decomposition behaviors. In Figure 7a, under the condition of 1.0 V/nm, the hydrate decomposition shows a layer-by-layer decomposition behavior. And under the condition of 1.5 V/nm, the hydrate exhibits a multilayer simultaneous decomposition behavior, as depicted in Figure 7b. This multilayer decomposition pattern makes the hydrate decompose more rapidly at 1.5 V/nm, which provides an effective strategy for the rapid release of methane.

In addition, the diffusion coefficients of H_2O in the system without ZIF-8 and in the system with ZIF-8 and under applied electric fields of 0 V/nm and 0.5 V/nm were calculated to be 4.17×10^{-13}, 9.35×10^{-13} and 1.85×10^{-12} m^2/s, respectively. And the dual effects of ZIF-8 and cosine oscillating electric fields led to an enhancement of the diffusion coefficients by 4.42 times, which significantly increased the probability of hydrate cage formation from H_2O, thus promoting hydrate growth.

Downloaded from pubs.acs.org/enfuem/article-pdf/40/5/2571/6332305/ef5c05447.pdf by SOUTH CHINA UNIV OF TECHNOLOGY user on 02 November 2026

https://doi.org/10.1021/acs.energyfuels.5c05447
Energy Fuels 2026, 40, 2571−2581

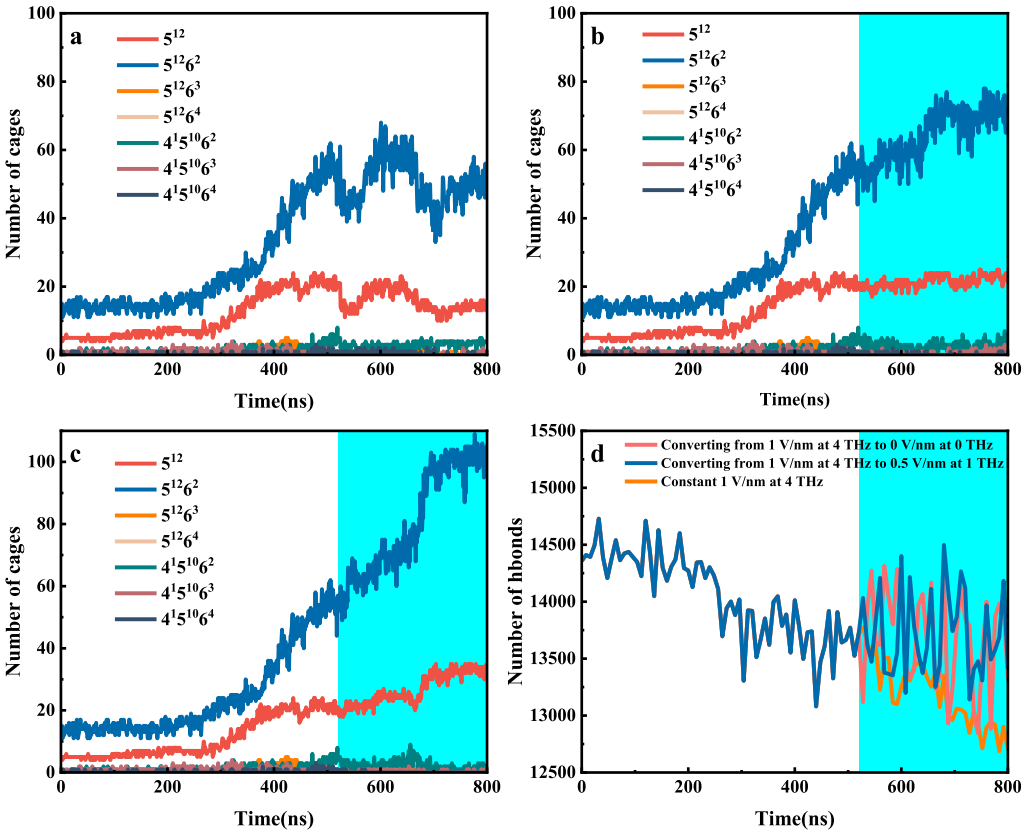


Figure 9. Variation of the number of ZIF-8 intergranular hydrate cages as well as the number of hydrogen bonds with time under different electric field application methods. (a) Constant application of 1.0 V/nm, 4.0 THz electric field; (b) 0 ns−522 ns applying 1.0 V/nm, 4.0 THz electric field, 522 ns−800 ns applying 0.5 V/nm, 1.0 THz electric field; (c) 0 ns−522 ns applying 1.0 V/nm, 4.0 THz electric field, 522 ns−800 ns not applying electric field. (d) Variation of hydrogen bonding between ZIF-8 crystals with time under different electric field application methods. (The white area is 1.0 V/nm, 4.0 THz, and the cyan area is the simulation after changing the electric field).

3.3. Effect of Electric Field Frequency on the Growth of ZIF-8 Intergranular Methane Hydrate

In addition to electric field strength, frequency plays a crucial role in adsorption hydration. The impact of the frequency (1.0−6.0 THz) of the cosine oscillating electric field on hydrate growth was analyzed under a 1.0 V/nm field and compared to the system without an electric field. Figure 8 demonstrates the variation of hydrate cage and F4 order parameters with time during the simulation. As can be seen from Figure 8a, frequencies between 2.0 and 5.0 THz promote hydrate formation. At frequencies of 1.0 THz or 6.0 THz, the electric field exerts a pronounced inhibitory influence, resulting in hydrate breakdown. This suggests that, under a given field strength, only certain frequency ranges are favorable for hydrate formation; exceeding these ranges leads to suppression.

The optimal electric field strength and frequency for hydrate growth depend on their combined coordination, rather than being fixed individually. At an electric field strength of 1.0 V/nm, the frequency that promotes methane hydrate growth in the intercrystalline ZIF-8 is 2.0−5.0 THz. However, the frequency promoting methane hydrate growth shifts to 1.0−2.0 THz when the electric field strength is 0.5 V/nm, as shown in Figure S5. Obviously, with stronger electric fields, the lowest frequency capable of stimulating hydrate formation shifts upward. However, when the frequency is too large, the hydrate appears to be unstable. As shown in Figure 8b, it can be seen that when the electric field frequency is increased to 4 THz and 5 THz, the F4 order parameter shows a rapid decrease at 522 ns, which suggests that the higher frequency electric field disrupts the ordered arrangement of water molecules, leading to the decomposition of methane hydrate.

Fang et al.[47] showed that high-frequency terahertz electric fields can resonate with H_2O, destroying the hydrogen bond between H_2O and reducing the surface tension. This increases the solubility of CH_4 and improves favorable environmental conditions for the growth of methane hydrates. This also explains the phenomenon of rapid decomposition of hydrates under a high-frequency electric field and then growing again. The calculation results of the mean-square displacement similarly proved this phenomenon, as shown in Figure S6. Between 400 and 500 ns, the mean-square displacement of H_2O rises sharply, indicating resonance with the electric field, intensifying H_2O motion and causing hydrate decomposition. However, the violent motion of H_2O also led to the disruption of hydrogen bonding in liquid water, enhancing the contact between CH_4 and H_2O, which in turn promoted the growth of hydrate. It can be seen that the growth of hydrate exhibits complex behavior under a high-frequency electric field. Under the electric field of 1.0 V/nm and 4.0 THz, the growth of methane hydrate exhibits three stages: (a) Slow growth stage: the hydrate grows slowly. The vigorous motion of H_2O under high-frequency fields requires more time to adapt and align with the electric field's oscillation; (b) rapid growth stage: the water molecules adapt to the oscillation frequency of the electric field at this stage, and the degree of ordering is

Downloaded from pubs.acs.org/enfuem/article-pdf/40/5/2571/6332305/ef5c05447.pdf by SOUTH CHINA UNIV OF TECHNOLOGY user on 02 November 2026

https://doi.org/10.1021/acs.energyfuels.5c05447
Energy Fuels 2026, 40, 2571−2581

increased. The hydrate exhibits rapid growth, with a rate up to five times greater than under field-free conditions; (c) unstable stage: At this stage, resonance between the electric field and H_2O in the hydrate causes partial decomposition. The destruction of hydrogen bonds by the electric field enhances the dissolution of CH_4 and promotes the formation of new hydrates.

The growth process of hydrate under a high-frequency oscillating electric field is complicated, and it may be difficult for hydrate to exist stably. However, an appropriate increase in the frequency of the electric field can realize rapid hydrate growth. If it can be ensured that the generated hydrate is no longer decomposed, it will be able to greatly improve the methane storage rate. In addition to promoting the growth of hydrates, changing the electric field frequency can also effectively promote the decomposition of hydrates. When the electric field frequency is less than 1.0 THz or greater than 6.0 THz, hydrates show rapid decomposition behavior. This is consistent with the conditions mentioned earlier for high-frequency electric fields to promote desorption of ZIF-8. Thus, by adjusting the frequency of the electric field, a rapid release of ZIF-8 and methane from the hydrate can be realized.

3.4. Effect of Intermittent Electric Field on ZIF-8 Adsorption-Hydration Storage of Methane

As previously noted, higher frequencies lead to a significant acceleration in the growth of ZIF-8 intergranular hydrate. However, this also leads to the failure of the hydrate to stabilize at a later stage. Therefore, ensuring that the generated hydrate is no longer decomposed is the key to achieving rapid hydration. When the electric field resonates with H_2O, it also breaks the hydrogen bonds in the hydrate, which can lead to sudden hydrate decomposition. The solution is to weaken the electric field or remove it directly before the hydrate decomposes. Figure 9a–c shows that the system, subjected to a constant 1.0 V/nm electric field and 4.0 THz, experienced rapid hydrate decomposition at 522 ns. However, after removing the electric field or shifting the electric field to 0.5 V/nm, 1.0 THz, the hydrate not only did not appear to decompose but was also able to maintain a high growth rate. An interesting phenomenon is found here: earlier findings indicate that hydrate formation proceeds significantly faster when subjected to a 0.5 V/nm, 1.0 THz field, compared to a field-free environment. However, on the basis of a 1.0 V/nm, 4.0 THz electric field, the formation rate of hydrate after removing the electric field is higher than that after transforming to a 0.5 V/nm, 1.0 THz electric field. After transforming the electric field to 0.5 V/nm, 1.0 THz, the growth of the hydrate was suspended for a short period of time, although it was no longer decomposed. This is due to the fact that H_2O needs some time to readapt to the oscillating frequency of the new electric field, so the optimal growth rate can be achieved by directly removing the electric field instead. Figure 9d shows the temporal variation in hydrogen bonding among ZIF-8 crystal structures. At 1.0 V/nm and 4.0 THz electric field, the hydrogen bond count keeps decreasing. The quantity of hydrogen bonding continues to decrease even in the rapid hydrate formation stage, which indicates that the electric field greatly destroys the hydrogen bonds in the liquid water, thus enhancing the dissolution of methane and promoting the growth of hydrate in the early stage. Once the electric field was reduced or removed, the number of hydrogen bonds increased again, and H_2O rearranged to continue hydrate formation.

Table 1 provides a comparison of methane hydrate growth rates across various systems. Shi et al.[36] showed that a cosine oscillating electric field of 1.5 V/nm and 0.4 THz could increase the methane hydrate growth rate in the bulk system up to three times. This study shows that under a 1.0 V/nm, 4 THz electric field and ZIF-8, the methane hydrate growth rate increased 8.5 times compared to the bulk system, demonstrating the strong synergistic effect between ZIF-8 and the electric field. And the optimal electric field conditions for methane hydrate in ZIF-8 intergranular pores were changed, which might be due to the constraining effect of ZIF-8 on water molecules, which changed the vibrational frequency of water molecules.

Table 1. Comparison of Methane Hydrate Average Growth Rate in Different Systems

system	electric field conditions	multiple of the average growth rate of bulk phase methane hydrate
bulk system	-	1
bulk system + cosine oscillating electric field	1.5 V/nm, 0.4 THz	3 [36]
ZIF-8 system	-	1.7
ZIF-8 system + Cosine oscillating electric field	1 V/nm, 4 THz	8.5

Table 2 summarizes the results of CH_4 capture by hydrates at 800 ns simulated in this study. The results indicate that the methane capture by hydrate in the intergranular pores of ZIF-8 reaches its highest at 260 K and 10 MPa with the application of a 1.0 V/nm, 4.0 THz intermittent electric field condition, which even exceeds the methane capture at 260 K and 30 MPa under the no electric field condition. Methane capture was enhanced 4-fold compared to the condition without the

Table 2. Results of Hydrate Storage CH_4 Amounts at 260 K and Different Cosine Oscillating Electric Field Conditions

pressure(MPa)	electric field strength(V/nm)	electric field frequency(THz)	total number of CH_4 stored in hydrates
10	0	0	34
10	0.1	0.5	37
10	0.1	1.0	23
10	0.1	2.0	31
10	0.5	0.5	29
10	0.5	1.0	57
10	0.5	2.0	37
10	0.5	6.0	0
10	1.0	1.0	0
10	1.0	2.0	45
10	1.0	4.0	69
10	1.0	5.0	42
10	1.0	6.0	0
10	1.5	0.5	7
10	1.5	1.0	0
10	1.5	2.0	46
10	1.0 converted to 0.5	4.0 converted to 1.0	100
10	1.0 converted to no electric field	4.0 converted to no electric field	136
30	0	0	111in

Downloaded from pubs.acs.org/enfuem/article-pdf/40/5/2571/6332305/ef5c05447.pdf by SOUTH CHINA UNIV OF TECHNOLOGY user on 02 November 2026

https://doi.org/10.1021/acs.energyfuels.5c05447
Energy Fuels 2026, 40, 2571−2581

electric field at 260 K and 10 MPa. This suggests that the application of a cosine oscillating electric field significantly promotes CH_4 hydrate growth, thereby reducing the energy required to achieve high-pressure conditions. Moreover, using an intermittent electric field prevents energy waste from continuous field application, lowering costs and offering significant potential for practical use.

4. CONCLUSIONS

This study explores how a cosine-type oscillating electric field impacts the adsorption-hydration characteristics of ZIF-8. The results show that adjusting the strength and frequency of the cosine oscillating electric field can realize the efficient storage and rapid release of methane from ZIF-8 adsorption-hydration.

It was observed that exposure to a cosine oscillating electric field enhances the structural stability of ZIF-8. An electric field of 1 V/nm at 8 THz promoted methane desorption from ZIF-8, reducing the methane residual fraction from 77.7% to 5.4%. This provides a potential strategy for methane desorption from ZIF-8 under mild conditions. For CH_4 hydrate nucleated between ZIF-8 crystals, growth is governed by the coordination between field strength and frequency. There is an optimal frequency range for each electric field strength. The 1.0 V/nm and 4.0 THz electric field makes the growth rate of hydrate five times that of the system without electric fields. However, the interaction between the electric field and water molecules causes instability in the hydrate structure, resulting in repeated decomposition and regrowth. This work proposes to use intermittent electric fields to coordinate these two contradictory effects. The results indicate that removing the electric field prior to hydrate decomposition preserves its initial influence on water molecule orientation, while enabling the field to break hydrogen bonds and improve gas−liquid contact, thus supporting continuous and rapid hydrate growth.

In conclusion, the electric field-coupled ZIF-8 adsorption hydrate approach provides a promising new approach for the efficient storage and rapid release of methane. In addition, the electric field also affects other porous materials as well as promoters, while the mode of application of the electric field also has an important influence on the growth of hydrates. Future work can be further developed from these aspects to accelerate the realization of industrial applications of hydrate storage and transportation technologies.

■ ASSOCIATED CONTENT

Data Availability Statement

Data will be made available on request.

Supporting Information

The Supporting Information is available free of charge at https://pubs.acs.org/doi/10.1021/acs.energyfuels.5c05447.

> Radial distribution functions of ZIF-8 framework atoms with and without electric fields; time evolution of methane adsorption in hydrated ZIF-8 systems; methane desorption behavior under different electric field strengths and frequencies; mean square displacement and diffusion coefficients of CH_4 and H_2O in ZIF-8 and ZIF-8-free systems; electric field frequency effects on methane hydrate cage formation and decomposition; supplementary figures related to molecular dynamics simulation results (PDF)

■ AUTHOR INFORMATION

Corresponding Author

Shuanshi Fan − *School of Chemistry and Chemical Engineering, South China University of Technology, Guangzhou 510640, China; Key Laboratory of Fuel Cell Technology of Guangdong Province, Guangzhou 510640, China;* orcid.org/0000-0002-2227-7620; Email: ssfan@scut.edu.cn

Authors

Changle Li − *School of Chemistry and Chemical Engineering, South China University of Technology, Guangzhou 510640, China*

Yanhong Wang − *School of Chemistry and Chemical Engineering, South China University of Technology, Guangzhou 510640, China; Key Laboratory of Heat and Mass Transfer and Low-Carbon Conversion, Ministry of Education, Guangzhou 510640, China;* orcid.org/0000-0002-0059-8159

Xuemei Lang − *School of Chemistry and Chemical Engineering, South China University of Technology, Guangzhou 510640, China; Key Laboratory of Fuel Cell Technology of Guangdong Province, Guangzhou 510640, China;* orcid.org/0000-0002-3189-7290

Gang Li − *School of Chemistry and Chemical Engineering, South China University of Technology, Guangzhou 510640, China;* orcid.org/0000-0001-5197-3425

Complete contact information is available at: https://pubs.acs.org/10.1021/acs.energyfuels.5c05447

Author Contributions

Changle Li: Writing—original draft, Data curation, Conceptualization, Methodology. Shuanshi Fan: Writing—review and editing, Conceptualization, Methodology, Resources. Yanhong Wang: Validation, Supervision. Xuemei Lang: Project administration. Gang Li: Investigation.

Notes

The authors declare no competing financial interest.

■ ACKNOWLEDGMENTS

This work was supported by the National Natural Science Foundation of China (U25A20275).

■ REFERENCES

(1) Wang, G.; Zhang, Z.; Lin, J. Multi-energy complementary power systems based on solar energy: A review. *Renew. Sustain. Energy Rev* **2024**, *199*, 114464.

(2) Liu, J.; Li, R.; Li, S.; Meucci, A.; Young, I. R. Increasing wave power due to global climate change and intensification of Antarctic Oscillation. *Appl. Energy* **2024**, *358*, 122572.

(3) Khan, N.; Kalair, A.; Abas, N.; Haider, A. Review of ocean tidal, wave and thermal energy technologies. *Renew. Sustain. Energy Rev* **2017**, *72*, 590−604.

(4) Chen, S.; Wang, Y.; Fan, S.; Lang, X.; Li, G. An innovative nucleation method for high and rapid hydrogen storage based on clathrate hydrates. *J Mater Chem A* **2024**, *12* (19), 11424−11438.

(5) Khan, I.; Zakari, A.; Zhang, J.; Dagar, V.; Singh, S. A study of trilemma energy balance, clean energy transitions, and economic expansion in the midst of environmental sustainability: New insights from three trilemma leadership. *Energy* **2022**, *248*, 123619.

(6) Popkova, E. G.; Sergi, B. S. Energy efficiency in leading emerging and developed countries. *Energy* **2021**, *221*, 119730.

Downloaded from pubs.acs.org/enfuem/article-pdf/40/5/2571/6332305/ef5c05447.pdf by SOUTH CHINA UNIV OF TECHNOLOGY user on 02 November 2026

(7) Dorokhov, V. V.; Nagibin, P. S.; Shlegel, N. E.; Strizhak, P. A. Using methane hydrate to intensify the combustion of composite slurry fuels. *Fuel* **2024**, *372*, 132247.
(8) Gaidukova, O. S.; Dorokhov, V. V.; Misyura, S. Y.; Morozov, V. S.; Shlegel, N. E.; Strizhak, P. A. Co-combustion of methane hydrate and conventional fuels. *Fuel* **2023**, *344*, 128046.
(9) Veluswamy, H. P.; Kumar, A.; Seo, Y.; Lee, J. D.; Linga, P. A review of solidified natural gas (SNG) technology for gas storage via clathrate hydrates. *Appl. Energy* **2018**, *216*, 262−285.
(10) Wang, S.; Xu, J.; Fan, S.; Wang, Y.; Lang, X.; Yu, C. Atmospheric preservation of CH^4 hydrate above ice point: A potential application for high-density natural gas storage under moderate conditions. *Fuel* **2021**, *293*, 120482.
(11) Sloan, E. D. Fundamental principles and applications of natural gas hydrates. *Nature* **2003**, *426* (6964), 353−359.
(12) Sloan, E. D., Jr.; Koh, C. A. *Clathrate Hydrates of Natural Gases*; CRC Press, 2007.p 752
(13) Chen, C.; Li, Y.; Cao, J. Methane Hydrate Formation in Hollow ZIF-8 Nanoparticles for Improved Methane Storage Capacity. *Catalysts* **2022**, *12* (5), 485.
(14) Chen, S.; Duan, J.; Xie, X.; Fu, Y.; Zi, M. Adsorption enhances CH_4 transport-driven hydrate formation in size-varied ZIF-8: Micro-mechanism for CH4 storage by adsorption-hydration hybrid technology. *Chem. Eng. J* **2024**, *482*, 148957.
(15) Duan, J.; Li, Q.; Fu, Y.; Chen, S.; Zhang, Y.; Liu, D. Accelerated formation of hydrate in size-varied ZIF-8 for CH_4 storage by adsorption-hydration hybrid technology. *Fuel* **2022**, *322*, 124266.
(16) Zhang, G.; Liu, Z.; Liu, D.; Lin, Y.; Wang, F. Hydrate-based adsorption-hydration hybrid approach enhances methane storage density in ZIF-8@AC. *Chem. Eng. J* **2023**, *455*, 140503.
(17) Zhou, L.; Sun, Y.; Zhou, Y. Enhancement of the methane storage on activated carbon by preadsorbed water. *AIChE J.* **2002**, *48* (10), 2412−2416.
(18) Andres-Garcia, E.; Dikhtiarenko, A.; Fauth, F.; Silvestre-Albero, J.; Ramos-Fernández, E. V.; Gascon, J.; et al. Methane hydrates: Nucleation in microporous materials. *Chem. Eng. J* **2019**, *360*, 569−576.
(19) Mallek, R.; Miqueu, C.; Jacob, M.; Dicharry, C. Investigation on hydrate formation from cyclopentane-loaded porous activated carbon particles. *Chem. Eng. Sci.* **2022**, *257*, 117714.
(20) Denning, S.; Lucero, J. M.; Majid, A. A. A.; Crawford, J. M.; Carreon, M. A.; Koh, C. A. Porous Organic Cage CC3: An Effective Promoter for Methane Hydrate Formation for Natural Gas Storage. *J. Phys. Chem. C* **2021**, *125* (37), 20512−20521.
(21) Li, D.-z.; Chen, L.; Liu, G.; Yuan, Z.-y.; Li, B.-f.; Zhang, X.; et al. Porous metal-organic frameworks for methane storage and capture: status and challenges. *New Carbon Mater* **2021**, *36* (3), 468−496.
(22) Ursueguía, D.; Díaz, E.; Ordóñez, S. Metal-Organic Frameworks (MOFs) as methane adsorbents: From storage to diluted coal mining streams concentration. *Sci. Total Environ.* **2021**, *790*, 148211.
(23) Mu, L.; Liu, B.; Liu, H.; Yang, Y.; Sun, C.; Chen, G. A novel method to improve the gas storage capacity of ZIF-8. *J. Mater. Chem.* **2012**, *22* (24), 12246−12252.
(24) Denning, S.; Majid, A. A. A.; Crawford, J. M.; Wells, J. D.; Carreon, M. A.; Koh, C. A. Methane storage scale-up using hydrates & metal organic framework HKUST-1 in a packed column. *Fuel* **2022**, *325*, 124920.
(25) Denning, S.; Majid, A. A. A.; Lucero, J. M.; Crawford, J. M.; Carreon, M. A.; Koh, C. A. Metal-Organic Framework HKUST-1 Promotes Methane Hydrate Formation for Improved Gas Storage Capacity. *ACS Appl. Mater. Interfaces* **2020**, *12* (47), 53510−53518.
(26) Denning, S.; Majid, A. A. A.; Lucero, J. M.; Crawford, J. M.; Carreon, M. A.; Koh, C. A. Methane Hydrate Growth Promoted by Microporous Zeolitic Imidazolate Frameworks ZIF-8 and ZIF-67 for Enhanced Methane Storage. *ACS Sustainable Chem. Eng.* **2021**, *9* (27), 9001−9010.
(27) Kim, D.; Ahn, Y.-H.; Lee, H. Phase Equilibria of CO_2 and CH_4 Hydrates in Intergranular Meso/Macro Pores of MIL-53 Metal Organic Framework. *J. Chem. Eng. Data* **2015**, *60* (7), 2178−2185.
(28) Casco, M. E.; Rey, F.; Jordá, J. L.; Rudić, S.; Fauth, F.; Martínez-Escandell, M.; et al. Paving the way for methane hydrate formation on metal-organic frameworks (MOFs). *Chem. Sci.* **2016**, *7* (6), 3658−3666.
(29) Zhang, Z.; Kusalik, P. G.; Liu, C.; Wu, N. Methane hydrate formation in slit-shaped pores: Impacts of surface hydrophilicity. *Energy* **2023**, *285*, 129414.
(30) Liu, W. G.; Chen, B. B.; Yang, M. J.; Wang, D. Y.; Song, Y. C. The Influence of Weak Electric Field on the THF Hydrate Formation Characteristics. *Kung Cheng Je Wu Li Hsueh Pao* **2019**, *40* (12), 2763−2768.
(31) Meng, Z.; Xu, J.; Hao, Y.; Chen, J.; Wang, B.; Zhang, X.; et al. Molecular study on the behavior of CO_2 hydrate growth promoted by the electric field. *Geoenergy Sci. Eng.* **2023**, *221*, 111261.
(32) Xu, J.; Yang, X.; Chen, J.; Meng, Z.; Wang, X.; Wang, B.; et al. Molecular study on the growth mechanism of CO_2-H_2 binary hydrate promoted by electric field. *Fuel* **2024**, *363*, 130924.
(33) Li, J.; Shi, L.; He, Y.; Lu, J.; Long, Z.; Liang, D. Kinetic characteristics of methane hydrate formation under the synergistic effect of electric field and Hexadecyl trimethyl ammonium Bromide. *Energy* **2023**, *283*, 129161.
(34) Zhou, T.; Liu, J.; Zhang, Y.; Jia, T.; Liu, S. Molecular mechanisms of methane hydrate dissociation under static and oscillating electric fields. *J. Mol. Liq.* **2026**, *441*, 129070.
(35) Liang, Y.; Bi, X.; Zhao, Y.; Tian, R.; Zhao, P.; Fang, W.; et al. Rapid decomposition of methane hydrates induced by terahertz bidirectional pulse electric fields. *Energy* **2024**, *286*, 129633.
(36) Shi, L.; Li, J.; Chen, Y.; Lu, J.; He, Y.; Liang, D. Molecular dynamics simulation study of the cosine oscillation electric field's effect on methane hydrate growth. *Energy* **2024**, *290*, 130240.
(37) Hao, Y.; Xu, J.; Yuan, S.; Meng, Z.; Wang, X.; Xue, J.; et al. Molecular dynamics study of electric field enhanced hydrate growth for gas storage. *J. Nat. Gas Sci. Eng.* **2022**, *103*, 104617.
(38) Luis, D. P.; López-Lemus, J.; Maspoch, M. L.; Franco-Urquiza, E. A.; Saint-Martin, H. Methane hydrate: shifting the coexistence temperature to higher temperatures with an external electric field. *Mol. Simul.* **2016**, *42* (12), 1014−1023.
(39) Xu, T.; Lang, X.; Fan, S.; Wang, Y.; Chen, J. The effect of electric fields in methane hydrate growth and dissociation: A molecular dynamics simulation. *Comput. Theor. Chem* **2019**, *1149*, 57−68.
(40) English, N. J.; MacElroy, J. M. D. Theoretical studies of the kinetics of methane hydrate crystallization in external electromagnetic fields. *J. Chem. Phys.* **2004**, *120* (21), 10247−10256.
(41) Waldron, C. J.; English, N. J. System-density fluctuations and electro-dissociation of methane clathrate hydrates in externally-applied static electric fields. *J. Chem. Thermodyn.* **2018**, *117*, 68−80.
(42) Chen, B.; Li, K.; Sun, H.; Jiang, L.; Yang, M.; Song, Y. Promoting Effect of Common Marine Cations on Hydrate Dissociation and Structural Evolution under a Static Electric Field. *J. Phys. Chem. B* **2023**, *127* (3), 698−709.
(43) Li, Z.; Lyu, M.; Jónsson, H.; Rose-Petruck, C. Observation of Electric-Field-Induced Liberation of Guest Molecules from Clathrate Hydrate. *J. Phys. Chem. Lett.* **2021**, *12* (42), 10410−10416.
(44) Ghaani, M. R.; English, N. J. Molecular Dynamics Study of Propane Hydrate Dissociation: Nonequilibrium Analysis in Externally Applied Electric Fields. *J. Phys. Chem. C* **2018**, *122* (13), 7504−7515.
(45) Luis, D. P.; Herrera-Hernandez, E. C.; Saint-Martin, H. A theoretical study of the dissociation of the sI methane hydrate induced by an external electric field. *J. Chem. Phys.* **2015**, *143* (20), 204503.
(46) Cao, P.; Sheng, J.; Andersen Sveinsson, H.; Wu, J.; Ning, F. Electric Field-Controlled Structural Instability and Mechanical Properties of Methane Hydrates. *Cryst. Growth Des.* **2022**, *22* (5), 3107−3118.

Downloaded from pubs.acs.org/enfuem/article-pdf/40/5/2571/6332305/ef5c05447.pdf by SOUTH CHINA UNIV OF TECHNOLOGY user on 02 November 2026

https://doi.org/10.1021/acs.energyfuels.5c05447
Energy Fuels 2026, 40, 2571−2581

(47) Fang, W.; Liang, Y.; Zhang, X.; Xie, Z.; Qu, Y.; Wang, Y.; et al. Gas solubility enhancement and hydrogen bond recombination regulated by terahertz electromagnetic field for rapid formation of gas hydrates. *Sep. Purif. Technol.* **2024**, *349*, 127830.
(48) Park, K. S.; Ni, Z.; Côté, A. P.; Choi, J. Y.; Huang, R.; Uribe-Romo, F. J.; et al. Exceptional chemical and thermal stability of zeolitic imidazolate frameworks. *Proc. Natl. Acad. Sci. U. S. A.* **2006**, *103* (27), 10186−10191.
(49) De Zitter, E.; Perl, D.; Savko, M.; Paley, D. W.; Thom, A. J.; Jeangerard, D.; et al. Elucidating metal-organic framework structures using synchrotron serial crystallography. *CrystEngComm* **2024**, *26* (39), 5644−5654.
(50) Zhang, G.; Sun, M.; Liu, B.; Wang, F. Adsorption-induced two-way nanoconvection enhances nucleation and growth kinetics of methane hydrates in confined porespace. *Chem. Eng. J* **2020**, *396*, 125256.
(51) Wang, Z.; Duan, J.; Chen, S.; Fu, Y.; Zhang, Y.; Wang, D.; et al. Molecular insights into hybrid CH_4 physisorption-hydrate growth in hydrophobic metal-organic framework ZIF-8: Implications for CH4 storage. *Chem. Eng. J* **2022**, *430*, 132901.
(52) Li, Z.; Li, N.; Kan, J.; Liu, B.; Chen, G. Competitive and synergistic mechanisms of adsorption-hydration during methane storage in the wet ZIF-8 fixed bed. *Fuel* **2023**, *351*, 129055.
(53) Lu, T. *Sobtop:A Tool of Generating Forcefield Parameters and GROMACS Topology File*, Version 1.0(dev5), Beijing Kein Research Center for Natural Sciences.http://sobereva.com/soft/Sobtop (accessed on Nov 18, 2024).
(54) Lu, T.; Chen, Q. Partial Charges. *Exploring Chemical Concepts Through Theory and Computation*; ed.; Liu, S., Ed.; Wiley-VCH GmbH, 2024, pp 161−188.
(55) Abascal, J. L. F.; Sanz, E.; Fernández, R. G.; Vega, C. A potential model for the study of ices and amorphous water: TIP4P/Ice. *J. Chem. Phys.* **2005**, *122* (23), 234511.
(56) Martin, M. G.; Siepmann, J. I. Transferable potentials for phase equilibria. 1. United-atom description of n-alkanes. *J. Phys. Chem. B* **1998**, *102* (14), 2569−2577.
(57) Fan, S.; Wu, S.; Lang, X.; Wang, Y.; Li, G. Insights of kaolinite surface and salt ions on the formation of carbon dioxide hydrates in confined nanopore: A molecular dynamics simulation study. *Gas Sci. Eng.* **2024**, *129*, 205390.
(58) Jiménez-Ángeles, F.; Firoozabadi, A. Enhanced Hydrate Nucleation near the Limit of Stability. *J. Phys. Chem. C* **2015**, *119* (16), 8798−8804.
(59) Wang, J.; Li, Z. Electric field modulated configuration and orientation of aqueous molecule chains. *J. Chem. Phys.* **2024**, *161* (9), 094305.
(60) Wu, Y.; Wang, Z.; Li, S.; Su, J. Terahertz electric field induced melting and transport of monolayer water confined in double-walled carbon nanotubes. *Phys. Chem. Chem. Phys.* **2024**, *26* (14), 10919−10931.
(61) Cassone, G.; Martelli, F. Electrofreezing of liquid water at ambient conditions. *Nat. Commun.* **2024**, *15* (1), 1856.

Downloaded from pubs.acs.org/enfuem/article-pdf/40/5/2571/6332305/ef5c05447.pdf by SOUTH CHINA UNIV OF TECHNOLOGY user on 02 November 2026

https://doi.org/10.1021/acs.energyfuels.5c05447
Energy Fuels 2026, 40, 2571−2581